SURFACE AND INTERFACE ANALYSIS
Surf. Interface Anal. 2005; **37**: 749–754
Published online in Wiley InterScience (www.interscience.wiley.com). DOI: 10.1002/sia.2075

SIA

XPS studies of octadecylphosphonic acid (OPA) monolayer interactions with some metal and mineral surfaces

N. S. McIntyre,[1]* H. - Y. Nie,[1] A. P. Grosvenor,[1] R. D. Davidson[1] and D. Briggs[2]

[1] Surface Science Western, Western Science Centre, The University of Western Ontario, London, Ontario N6A 5B7, Canada
[2] Centre for Surface Chemical Analysis, University of Nottingham, University Park, Nottingham NG7 2RD, UK

Received 29 April 2005; Revised 27 June 2005; Accepted 30 June 2005

Partial and complete self-assembled monolayers (SAMs) of octadecylphosphonic acid (OPA) have been deposited onto air-exposed surfaces of the metals copper, silver, gold, iron, silicon and aluminium, as well as onto freshly cleaved, air-exposed surfaces of the minerals muscovite and biotite. The line width of the C(1s) signal in the XPS spectra of the surface narrowed, as the extent of coverage increased to 100%, to a half-width of 0.9 eV. Moreover, the line widths associated with the insulating muscovite substrate also became substantially narrower as OPA coverage increased. Binding energy differences on this charge-shifted surface were found to be more consistent when OPA was used as a charge reference, compared to using adventitious carbon as a reference. OPA coverage of the air-exposed metals copper, silver, gold and iron also produced narrow C(1s) spectra whose binding energies were consistently close to 284.9 eV. The C(1s) binding energy positions on Al and Si samples were charge-shifted by the insulating nature of the thin oxide formed on air exposure, or by the insulating nature of the substrate in the case of the minerals. Correction of the observed C(1s) energy position to 284.9 eV gave sets of elemental binding energies for the substrate materials that were reproducible. Thus, OPA coverage could be a possible alternative candidate for use in charge correction of binding energies of insulating materials. The OPA coverage cases were modelled using the software QUASES™ Analyse. For the substrates copper, silver, gold, iron and aluminium, analyses of the metal core line spectra gave OPA overlayer thicknesses close to those measured by AFM (1.6 nm). However, QUASES™ analyses of the C(1s) extrinsic backgrounds for the same surfaces required the use of an attenuation length of only 0.4 nm to derive a comparable thickness – much lower than literature values for carbon. This discrepancy is ascribed to the structured nature of the SAM.

KEYWORDS: octadecylphosphonic acid (OPA); self-assembled monolayers (SAMs); x-ray photoelectron spectroscopy (XPS); atomic force microscopy (AFM)

INTRODUCTION

Our recent studies of OPA (octadecylphosphonic acid) SAMs (self-assembled monolayers) have led to a fairly straightforward protocol for deposition of complete monolayers on many hydrophilic surfaces.[1] The resultant SAM consists of an array of nearly vertical OPA molecules with the phosphate head group bonded to the substrate and the end of the long-chain hydrocarbon tail providing the new hydrophobic surface. The possibility of creating such structures has raised the question that these layers might be used for energy calibration of photoelectron spectra from insulating materials.

The long-chain tail is attractive for use as a binding energy reference. Most carbons within the chain should experience the same potential, thereby presenting a peak that is little broadened by chemical effects. Moreover, the regular structure of a SAM that completely covers the substrate will encourage an even distribution of any charge that results from irradiation of an insulating substrate. Electrical contact between the substrates is established by the strong ionic/covalent bond formed between the phosphate head group and any hydrophilic surface, including most of the native oxides formed on metal surfaces. Such a carbon-chain model as a charge reference is to be preferred to the unknown, and, presumably, heterogeneous carbon structures that form as a result of exposure of clean surfaces to the atmosphere, otherwise known as *adventitious carbon*.[2] Carbon(1s) spectra from adventitious carbon are seldom symmetric and have a half-width usually in excess of 1.3 eV, under spectrometer resolution conditions capable of producing an $Ag(3d_{5/2})$ half-width of <0.6 eV. Moreover, the position of the adventitious carbon peak has been shown to be influenced by the electronic structures of the substrate surface, particularly in the case of metals.[3] It might be expected that, for OPA

*Correspondence to: N. S. McIntyre, Surface Science Western, Room G-1, Western Science Centre, The University of Western Ontario, London, Ontario N6A 5B7, Canada. E-mail: smcintyr@uwo.ca

monolayers, the C(1s) line position for carbon atoms over 1 nm distant from the substrate would experience less influence from changes in the electronic distribution at the original surface.

The present paper shows that, in fact, the C(1s) line for OPA layers on metals has a well-defined and narrow peak shape that appears to be reproducibly sensitive to charge-induced shifts in peak positions on a number of insulating surfaces. Further, a curious quality of the OPA monolayers was discovered as a result of a QUASES™ analysis of the spectra involving the overlayers. These overlayers are shown to have much lower attenuation lengths, compared to expected attenuation length values for carbon from the literature.

EXPERIMENTAL

Monolayer films of OPA (Alfa Aesar, Ward Hill, Massachusetts, USA) were spin-coated onto 2 cm^2 areas of freshly cleaved mica (muscovite) (Bancroft, Ontario, Canada) and biotite (Bancroft, Ontario, Canada). Deposits were also made onto similar areas of polished (0.25 micron diamond) metal specimens of high purity, such as polycrystalline silver, copper and gold. X-ray photoelectron spectroscopy (XPS) spectra showed the presence of oxide layers on the silver and copper surfaces after polishing, while it showed the presence of an oxygen adsorbate on the gold surface. Thin films (~0.1 μm) of iron and aluminium metals were deposited *in vacuo* by radiofrequency plasma onto surfaces of single crystal Si(110). These metallic surfaces, on exposure to air, produced thin oxide surfaces of haematite and amorphous aluminium oxyhydroxide, respectively. OPA films were also cast onto these surfaces. Finally, a substrate of Si(100) was oxidised briefly in a UV/ozone atmosphere to oxidise the surface to a depth of several nanometres, and it was also coated with OPA.[1]

Samples of gold, silver and copper were all spin-coated with OPA directly after polishing and ultrasonic cleaning in methanol. In addition, a select area of each of the metal surfaces was sputter-cleaned by ion bombardment and these samples were brought back into the ambient air vacuum and spin-coated with OPA. XPS spectra were obtained on sputtered and non-sputtered areas, before and after coating with OPA.

All specimens were coated with an OPA layer in air using the same protocol deemed suitable for the deposition of OPA SAMs on muscovite.[1] This process uses reagent grade chloroform as the delivery medium.

It was possible to measure the OPA coverage of muscovite, biotite and the SiO_2 thick film and thin film oxides on iron, silicon and aluminium by atomic force microscopy (AFM) using a Topometrix Explorer. It was possible to measure the extent of surface coverage of the OPA from the image contrast, to a precision of ±8%. In the case of muscovite, coverage ranging from 10 to 100% could be produced by changing the concentration of OPA added to the carrier solvent. Other surfaces studied were too rough to be measured by AFM; full coverage for equivalent doses of OPA solution was assumed, on the basis of the observations for those smooth surfaces whose coverage could be measured by AFM.

XPS measurements were made with a Kratos AXIS Ultra spectrometer using Al K_α monochromatised radiation. High-resolution spectra were acquired with a pass energy of 10 eV. An area ~700 × 300 μm in diameter was analysed in each case using a normal take-off angle. QUASES™ analysis[4,5] of spectra was conducted using the QUASES™ Analyse program on a broad-range spectra collected with 2000 points across a 1100-eV range. For the three substrates studied, the attenuation length for iron oxide was obtained experimentally (reported in a previous publication[6] from this laboratory). The attenuation length for silver and silicon were calculated as inelastic mean free paths using the TPP calculator in the QUASES™ software. The universal cross section was used for iron oxide and silver, while a specific cross section was taken from the software for silicon. For insulating specimens, the Kratos compensating flood gun was used. Quantitation of XPS spectra was carried out using integrated photoelectron peak intensities, corrected for photoelectron cross section using the Kratos-supplied sensitivity factors. Quantitative results were expressed as if the surface had a semi-infinite thickness. Thus, in many the following measurements where the carbon is primarily confined to the outermost 2 nm, the percent carbon values should be used only as a measure of the increase in carbon relative to other elements within the substrate.

RESULTS AND DISCUSSION

Muscovite surfaces were analysed with several different coverages of OPA. The AFM images of four different coverages (20, 70, 90 and 100%) are shown in Fig. 1. The coverage gradually changes from isolated islands, to coalesced islands, to almost complete coverage (except for sub-micron bare spots), to complete coverage. These and other coverages of cleaved muscovite were analysed by XPS; several different areas of each sample were analysed. A plot of the C(1s) carbon 'concentration' on freshly cleaved muscovite *versus* OPA coverage, as determined by AFM, is shown in Fig. 2. The carbon concentration at 0% coverage can be considered to be due to adventitious carbon that formed on the surface immediately following cleaving. As OPA coverage is increased, the carbon concentration increases in intensity in a quasi-linear fashion, with 35% carbon representing the coverage of the surface by an array of hydrocarbon molecules 18 carbons in length. It is surprising that this complete SAM has only a modest effect in attenuating electrons from the elements in the substrate. Further discussion on this will appear later in the text.

Figure 3 shows the binding energy region near the C(1s) line position for muscovite specimens that were freshly cleaved, or cleaved and covered with 70 and 90% coverages of OPA. The C(1s) half-width for the freshly cleaved specimen (Fig. 3(a)) is close to 1.2 eV; however, with addition of the OPA overlayer, the half-width reduces to 0.93 eV, then to 0.90 eV. The C(1s) line width (~0.9 eV) of the OPA itself is comparable to line widths obtained for other thin film polymers cast onto conducting substrates.[7] Thus, the carbon in the overlayer presents a more homogeneous type of carbon than the adventitious carbon on the cleaved muscovite

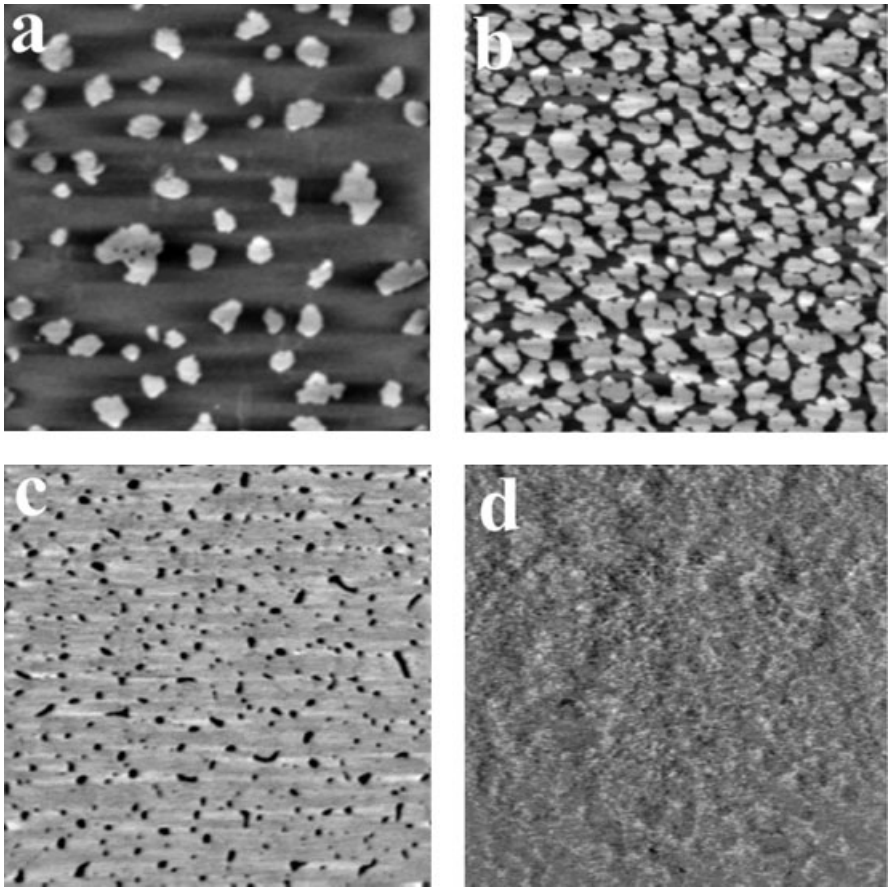

Figure 1. Grey-scale AFM topographic images (scan area: 1.5 × 1.5 μm) of four different OPA coverages on a surface of freshly cleaved muscovite: (a) 20% coverage, (b) 70% coverage, (c) 90% coverage, and (d) 100% coverage. In (a–c), the darker shading represents the substrate. The height range for (a) and (b) is 2.5 nm. The image in (c) shows a smaller height range of 1.3 nm as the pit size becomes small enough to convolute with the AFM tip. The morphology in (d) has a height range of 0.4 nm, showing a featureless surface with a corrugation height of a couple of angstroms.

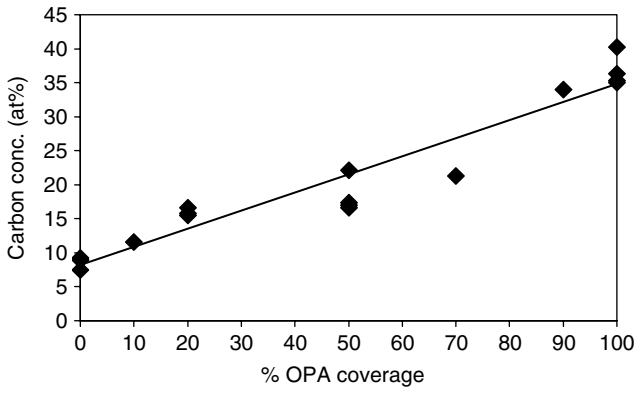

Figure 2. Relationship between C(1s) carbon 'concentration' (filled diamonds) and the OPA coverage of a surface of freshly cleaved muscovite. The dark line indicates a linear least squares fit to the plot.

surface. For surfaces with >90% coverage of OPA, the measured difference between the C(1s) centroid and the K($2p_{3/2}$) line was 8.23 ± 0.02 eV for seven different areas, whereas for the uncoated muscovite surface the difference was 8.03 ± 0.03 eV for eight different areas. A coverage of 50% OPA produced a difference of 8.18 ± 0.07 eV; the lower precision is perhaps a result of local variations in the coverage. Thus, there would be a difference of 0.2 eV in the binding energy of the K($2p_{3/2}$) line referenced to the OPA SAM compared to a reference to adventitious carbon. The half-widths of the K(2p) line from the muscovite also undergo significant narrowing when the OPA is applied from a half-width of 1.30 eV uncoated to 1.10 eV after 100% coating.

The same deposition protocol onto cleaved biotite surfaces also produced complete coverages that generated C(1s) spectra with line widths that were as narrow as those found for the layer on muscovite. In this case, the measured difference between the C(1s) centroid and that of the K($2p_{3/2}$) line was 8.35 eV for two measurements. Core line spectral half-widths were also narrowed for biotite following coverage with OPA.

The narrowing of core line peaks associated with the insulating mineral substrates, along with the C(1s) line for the OPA, could result from the lessening of any differential charging, as the surface is gradually covered with a layer that creates the same charging condition everywhere. The C(1s) line shape for OPA is probably also inherently narrower than that for adventitious carbon because the latter could be associated with multiple species (or electronic contacts). Coverage of such insulating surfaces with OPA

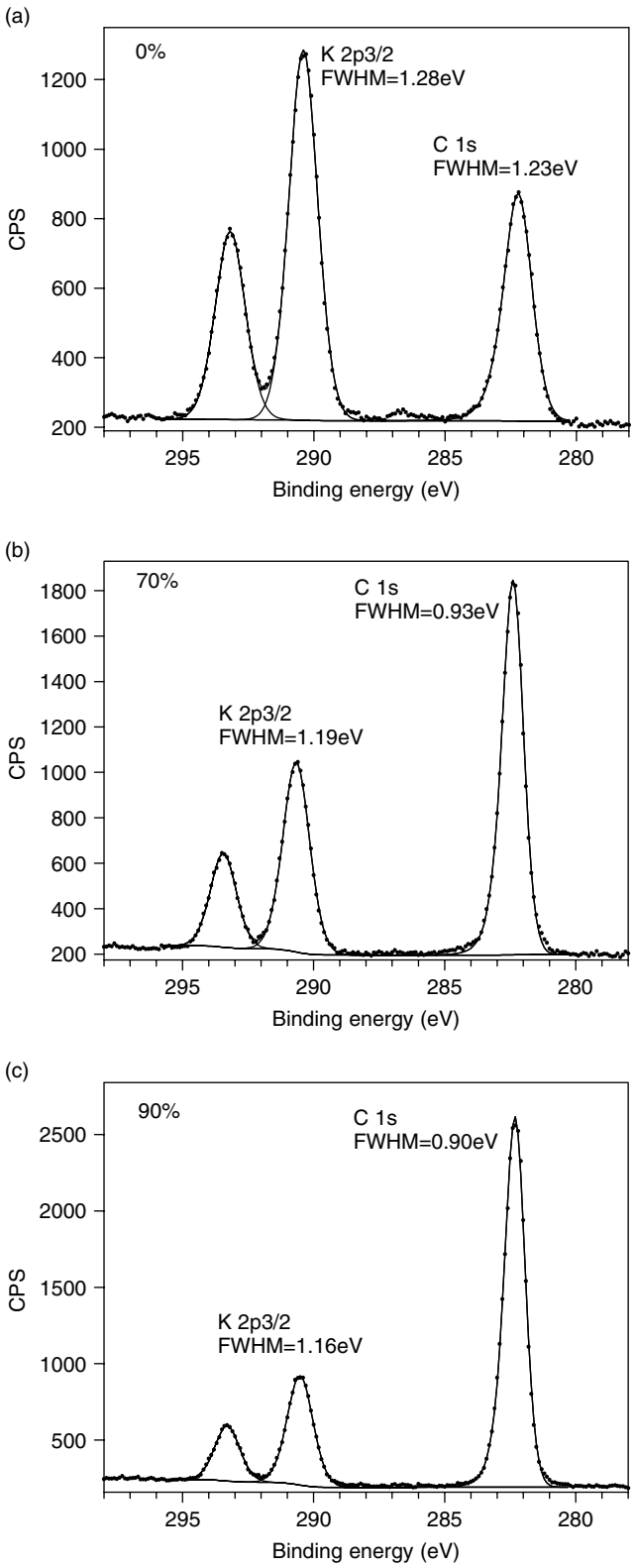

Figure 3. Spectra of the C(1s) and K(2p) binding energy region for: (a) a freshly cleaved surface of muscovite, (b) cleaved muscovite with a 70% coverage of OPA and, (c) cleaved muscovite with a 90% coverage of OPA. Flood gun compensation of the surface was used during spectral collection.

monolayers could well prove to be beneficial in controlling line-broadening for a large number of insulating materials.

The metals Fe, Cu, Ag, Al, Si and Au were coated with OPA SAMs; they were then studied by AFM and XPS. It was possible to measure OPA coverages of the Fe, Al and Si surfaces because they were made on a single crystal silicon substrate. In each of these cases, it was possible to confirm, using AFM, that the OPA coverage of the surface was 90% or greater. The extent of coverage on the Cu, Ag and Au surfaces could not be determined by AFM because of the rough substrate; however, all of these surfaces exhibited very hydrophobic behaviour. In Table 1, the pertinent XPS data are shown for all these samples, including the line positions and the half-widths for the C(1s) peak of the original adventitious carbon layer on the surface, the OPA overlayer, and the positions and half-widths for the metal substrate, as well as for any oxide present. For as received gold, the C(1s) binding energy for adventitious carbon on the surface was 285.2 eV, whereas, for an OPA-covered surface, the binding energy was 285.0 eV. The C(1s) line width for the OPA overlayer was narrower than that for the adventitious overlayer, but was still broader than what was observed on the muscovite and biotite surfaces. The gold surface was sputtered and again coated with OPA; the resultant C(1s) line had a small, but significant, upward shift in binding energy to 285.1 eV. The C(1s) peak for the OPA coating on silver was narrower, and its binding energy of 284.9 eV lay closer to that observed for the OPA coating on gold. The adventitious carbon binding energies on gold and silver are several tenths of an eV apart, possibly as a result of significant electronic interaction with the different substrates.[2] Coverage of polished copper with an OPA film resulted in a C(1s) peak at 284.9 eV, while on oxidised iron, the OPA C(1s) peak was at 284.8 eV. Therefore, the binding energy of the OPA film, while not totally invariant, seems to be more consistent than the values found for adventitious carbon. Sputtering of the metal surface, followed by OPA coating, also produces a similar set of fairly consistent binding energies.

It is interesting to know that the half-width of the OPA C(1s) line for these relatively rough metal surfaces is measurably broader than those for the atomically flat muscovite and biotite surfaces. On the rough metal surfaces, the local work function could vary according to the density of kink or step sites on the surface; on the muscovite surface, the density of these sites would be considerably lower than that on the metals studied.

On the basis of experiments on these four metal surfaces, the average C(1s) value for an OPA overlayer was found to be 284.95 ± 0.15 eV. The binding energies for charge-shifted aluminium oxide and silicon oxide peaks in Table 1 would thereby be corrected to 74.1 eV and 102.7 eV, respectively, using OPA as a reference. These values are lower than average literature binding energies for these species: Al_2O_3, 74.5 ± 0.2 eV; SiO_2, 103.4 ± 0.3 eV.[8]

The somewhat broader C(1s) line found for OPA deposited on these metal surfaces could result from the range of different electronic interactions of OPA with the more complex metal/thin film oxide structures, compared to interactions with those on the layered mineral surfaces.

On substrates where a total coverage by an OPA monolayer can be assured, the layer can be used to determine

Table 1. Binding energies for surface carbon species and for their metal substrates. The peak widths (FWHM) are given in brackets

Surface phase prepared	C(1s) BEs (FWHM) (eV)	Substrate BEs (eV)
Polished gold	285.2 (1.16)	Au($4f_{7/2}$): BE = 84.0 (0.71)
Polished gold + OPA	285.0 (1.00)	Au($4f_{7/2}$): BE = 84.0 (0.71)
Sputtered gold	–	Au($4f_{7/2}$): BE = 84.0 (0.74)
Sputtered gold + OPA	285.1 (1.1)	Au($4f_{7/2}$): BE = 84.0 (0.71)
Polished silver	284.7 (1.21)	Ag($3d_{5/2}$): BE = 368.2 (1.01)
Polished silver + OPA	285.1 (1.00)	Ag($3d_{5/2}$): BE = 368.2 (0.69)
Sputtered silver	–	Ag($3d_{5/2}$): BE = 368.2 (0.69)
Sputtered silver + OPA	284.9 (1.06)	Ag($3d_{5/2}$): BE = 368.2 (0.98)
Polished copper	285.3 (1.26)	Cu($2p_{3/2}$): BE = 932.5 (1.08); 934.9 (2.60)
Polished copper + OPA	284.9 (1.19)	Cu($2p_{3/2}$): BE = 932.5 (1.10)
Sputtered copper	–	Cu($2p_{3/2}$): BE = 932.6 (0.98)
Sputtered copper + OPA	284.9 (1.14)	Cu($2p_{3/2}$): BE = 932.6 (1.13); 935.0 (3.0)
Iron deposited on Si(III) + OPA	284.8 (1.06)	Fe($2p_{3/2}$): BE = 710.8 (oxides)
Aluminium deposited on Si(III) + OPA	286.7 (1.10)	Al($2p_{3/2}$): BE = 72.9; 75.9 (1.7) (oxide)
Si(III) + OPA, 60% coverage	286.4 (1.12)	Si($2p_{3/2}$): BE = 99.9; 104.1 (1.05) (oxide)
Si(III) + OPA, 100% coverage	286.1 (1.34)	Si($2p_{3/2}$): BE = 103.9 (105)

Table 2. OPA layer thicknesses determined by QUASES™ analysis of substrate photoelectron spectra

Substrate	Core line used	Attenuation length (nm)[a]	OPA thickness determined (nm)[b]	Attenuation length determined for C(1s) line (nm)
Fe_2O_3	Fe(2p)	1.41	1.65	0.5
Ag metal	Ag(3d)	1.542	1.6	0.4
Si (thin oxide)	Si(2p)	3.52	1.6	0.2

[a] Assumed equal to IMFP calculated from TPP.

[b] Experimentally determined using AFM.

the attenuation length for the C(1s) signal arising from the 18-carbon chain. This chain is oriented in a near-normal position with respect to the substrate. On a muscovite substrate the height of the OPA overlayer was determined by AFM to be 1.7 ± 0.2 nm, almost all of it consisting of the long-chain hydrocarbon. Although AFM has not yet been able to measure the OPA overlayer on an iron oxide owing to its 'rougher' surface, we assume that the OPA overlayer on the iron oxide has a similar thickness to that on a muscovite. On an oxidised iron surface, the thickness of the same OPA overlayer could also be determined by QUASES™ Analysis[9] using the universal loss function and an attenuation length of 1.4 nm[10] for the oxide. The resultant QUASES™ analysis of the Fe(2p) line shape (see Table 2) shows that the overlayer is 1.65-nm thick – a value in close agreement with the AFM measurement. A subsequent QUASES™ analysis of the C(1s) spectrum required the use of an attenuation length of 0.5 nm to give the same layer thickness as was found for the oxide. Thus, the attenuation length for vertically structured hydrocarbon chains on a surface is three to four times lower than the 3.8 nm value for linear hydrocarbons such as paraffin or polyethylene, as determined from TPP calculations.[10] Similar attenuation lengths were found for carbon on silicon and on silver surfaces. Therefore, the columnar structure of the OPA may focus on the electron trajectories. Aside from the theoretical interest in such a result, the very low attenuation length of the OPA increases its attractiveness for use as an energy calibration medium to measure surface charging. QUASES™ studies of our other systems were not attempted because of interferences from the extrinsic background of nearby lines.

CONCLUSIONS

(1) OPA overlayers on the insulating substrates studied give a consistent value for the surface charge-induced energy shift on the binding energy scale in the XPS spectra.
(2) OPA layers on a number of different metal (conducting) substrates give a mean value for the C(1s) binding energy of 284.9 ± 0.15 eV; some effects due to the electron density of each particular metal are still detected, but these are smaller than that observed for adventitious carbon. In addition, the C(1s) peak for the OPA overlayer is narrower, better defined and more reproducible than it is for adventitious carbon.
(3) The attenuation lengths for the C(1s) line of the overlayers derived from peak-shape analysis are considerably smaller than those predicted by TPP calculations.

REFERENCES

1. Nie H-Y, Walzak MJ, McIntyre NS. Surface Science Western, unpublished results, to be submitted to *J. Am. Chem. Soc.*
2. Miller DJ, Biesinger MC, McIntyre NS. *Surf. Interface Anal.* 2002; **33**: 299.
3. Castle JE, Salvi AM, Guaseito MR. *Surf. Interface Anal.* 1999; **27**: 753.
4. Tougaard S. *QUASES™: Software Package for Quantitative XPS/AES of Surface Nano-structures by Peak Shape Analysis*, version 4.4. University of Southern Denmark: Odense, Denmark, 2000.
5. Tougaard S. *Surf. Interface Anal.* 1998; **26**: 249.

6. Grosvenor AP, Kobe BA, McIntyre NS, Tougaard S, Lennard WN. *Surf. Interface Anal.* 2004; **36**: 632.
7. Beamson G, Briggs D. *High Resolution XPS of Organic Polymers – The Scienta ESCA300 Database*, vol. 56. Wiley: Chichester, 1992.
8. Wagner CD, Naumkin AV, Kraut-Vass A, Allison JW, Powell CJ, Rumble JR Jr. *NIST X-ray Photoelectron Spectroscopy Database*. NIST Standard Reference Database 20, Version 3.4 (Web Version), NIST: Washington, DC, 2003.
9. Kover L, Tougaard S, Werner WSM, Cserny I. *Surf. Interface Anal.* 2002; **33**: 681.
10. Cumpson PJ. *Surf. Interface Anal.* 2001; **31**: 23.